



## Elastic properties of boro-tellurite glasses doped with europium oxide

Chinnappareddy DEVARAJA<sup>1</sup>, G. V. Jagadeesha GOWDA<sup>1,\*</sup>, Bheemaiah ERAIAH<sup>2</sup>, and G. K. Narasihma MURTHY<sup>3</sup>

<sup>1</sup> Department of Physics, Sapthagiri College of Engineering, Bengaluru -560057, Karnataka, India

<sup>2</sup> Department of Physics, Bangalore University, Bengaluru-560056, Karnataka, India

<sup>3</sup> Department of Physics, Bangalore Institute of Technology, Bengaluru, Karnataka, India

\*Corresponding author e-mail: jagadeeshagowdagv@gmail.com

### Received date:

14 January 2022

### Revised date:

5 March 2022

### Accepted date:

17 March 2022

### Keywords:

Elastic modulus;  
Microhardness;  
Thermal expansion coefficient;  
Acoustic impedance;  
Fractional bond connectivity

### Abstract

The glass series of  $x\text{Eu}_2\text{O}_3\text{-}5\text{PbO-}25\text{TeO}_2\text{-(}70\text{-}x\text{) B}_2\text{O}_3$ , where  $x=0.1$  mol% to 0.6 mol% were prepared by employing the conventional melt quenching method. The non-crystallinity of prepared BTE glasses was examined by the X-ray diffraction method. The very important mechanical properties such as elastic moduli, Debye temperature, Poisson's ratio, fractional bond connectivity, softening temperature, acoustic impedance, and the thermal expansion coefficient of the BTE glasses have been studied by measuring ultrasonic velocity. The experimental results indicate that the calculated parameters strongly depend on increasing  $\text{Eu}_2\text{O}_3$  concentration. The elastic moduli of the prepared samples were found to decrease with  $\text{Eu}_2\text{O}_3$  concentration and this increases the discontinuity in the glass network.

## 1. Introduction

The ultrasonic non-destructive method is one of the best methods for evaluating mechanical properties, phase changes, and elastic moduli [1-4]. The elastic properties of solid materials are of considerable importance in the various experimental methods available to study structure-property relationships [5]. The transmission of ultrasonic waves in glass-like solids gives information about the solid-state motion of an object. Acoustic wave transmission in bulk glasses is of great attention to understand the mechanical properties [6]. Many physical parameters of the glasses, which are subjective to elastic moduli can be determined by using ultrasonic velocity [6-9]. Consequently, the choice of the most appropriate material for a specific application needs awareness of its mechanical properties [9-11].

Glasses having divalent ions such as  $\text{Te}^{2+}$ ,  $\text{Pb}^{2+}$  play a significant role in the modification of property [12-14]. It is perceived that the incorporation of metal oxides like  $\text{PbO}$ ,  $\text{ZnO}$  into the boro-tellurite glass matrix could do changes in the densities and molar volume of the glasses [14-16]. It is reported that tellurite ( $\text{TeO}_2$ ) converts  $\text{TeO}_4$  into  $\text{TeO}_{3+1}$  and  $\text{TeO}_3$  units when  $\text{B}_2\text{O}_3$  is added to the  $\text{TeO}_2$  glass network and it also improves the ability of glass formation with  $\text{TeO}_2$  [17,18]. The addition of  $\text{B}_2\text{O}_3$  decreases B-O coordination and increases  $\text{B}_2\text{O}_3$  concentration in boro-tellurite glasses. Boron oxide is an exceptional material for blending with tellurium oxide, which improves the quality of glass in terms of glass stability, transparency,

and hardness of rare-earth ions solubility. Borate-based specimens find widespread applications in all fields due to their various physical-chemical properties [19-21]. Additionally, it is shown that the elastic properties associated with acoustic properties are most useful due to their preferred applications in a few devices like light modulators and solid-state sensors [1-3,16,21,22].

Glasses embedded with rare-earth ions have great interest due to their broad range of applications such as temperature sensors, memory devices, solid-state lasers, infrared to visible up-converters, bulk lasers, planar waveguides, optical fiber amplifiers, high-density memory devices, flat plane displays, field emission displays, electroluminescent devices, optical data storage devices, color display devices [23-27]. The europium consists of energy level with simple structure and non-degenerate ground state  $^7\text{F}_0$  and emits  $^5\text{D}_0$  states. Hence the substitution of  $\text{Eu}^{3+}$  ions into the glass network is relatively advantageous to the study of disordered materials [28,29]. As per the literature survey, there is insufficient information regarding the effect of the addition of  $\text{Eu}^{3+}$  ions to the boro-tellurite matrix on mechanical properties. Therefore it is very motivating to discover the relation between the significant changes in the glass structure, the density, and mechanical properties of  $\text{Eu}^{3+}$  ions in boro-tellurite glasses.

In the current work, detailed information on the influence of europium oxide on density and elastic properties of boro-tellurite glasses were deliberated, and it also examined the structural conversion of the boro-tellurite system induced by the addition of  $\text{Eu}_2\text{O}_3$ .

## 2. Materials and methods

H<sub>3</sub>BO<sub>3</sub>, PbO, TeO<sub>2</sub>, and Eu<sub>2</sub>O<sub>3</sub> chemicals were procured from Sigma Aldrich with 99.9% purity and were taken as starting materials for glass sample making. The glass samples xEu<sub>2</sub>O<sub>3</sub>-5PbO-25TeO<sub>2</sub>-(70-x) B<sub>2</sub>O<sub>3</sub>, x=0.1 to 0.6 mol%, are made by the conventional melt quenching method. By proper and repeated grinding of the chemical mixture, fine powder was obtained. To obtain a uniform mixture the chemicals were stirred with a glass rod for about 30 min, then transferred to porcelain crucibles, and then heated in a muffle furnace. The mixture was dissolved in the crucible for about 1 h at 1150 K to homogenize the solvent. Glass samples were annealed for 2 h at 350 K to avoid mechanical stress developed through quenching. The obtained glasses are termed BTE1-6. The obtained glasses are colourless, transparent, and the glasses are well polished by P1500 grade emery paper to achieve the cylindrical shape of thickness around 10 mm.

Solubility was performed under controlled conditions with stirring periodically. The molten samples were cast in the size required for ultrasonic velocity measurements. The ready glass samples were polished and the outer surfaces were made completely horizontal. By using digital vernier calipers having an accuracy of about 0.0001 mm, the thickness of the BTE glasses was measured.

The non-crystallinity of obtained BTE glasses was confirmed by employing X-ray diffraction measurement. Cu K $\alpha$  radiations with wavelength 1.54 Å at 40 kV were used for the diffractometer. Diffraction radiations were collected by scintillation detector in the range of 10° to 80°.

Using acetone as a buoyant fluid, the density of specimens are measured by the Archimedes principle [6-8],

$$\rho = \frac{\rho_b \times W_a}{W_a - W_b} \quad (1)$$

Where W<sub>a</sub> is the weight of the specimen in air, W<sub>b</sub> is the weight of the specimen in buoyant liquid and  $\rho_b$  is the density of the buoyant liquid. Digital balance was used to weigh each sample. Using the molecular weights and density, the molar volume (V<sub>m</sub>) of the glass samples can be calculated by the relation [12,13],

$$V_m = \frac{M}{\rho} \quad (2)$$

Where M is the average molecular weight of the specimen and  $\rho$  is its density.

The ultrasonic longitudinal and shear velocities of the sample are measured by the pulse-echo procedure with the frequency of 2 MHz X-cut and Y-cut transducers. Ultrasonic velocity is measured by the V = 2d/t relation, where d denotes the thickness of the sample, t refers to the transit time and V is the ultrasonic velocity [3-7].

### 2.1 Theory and calculations

With the help of acquired values of longitudinal velocity (V<sub>1</sub>), shear velocity (V<sub>s</sub>), and density ( $\rho$ ) at room temperature, the different elastic modulus, and thermal properties were calculated by using mathematical relations [9,30-32] as shown here:

Longitudinal modulus (L)

$$L = \rho V_1^2 \quad (3)$$

Shear modulus (G)

$$G = \rho V_s^2 \quad (4)$$

Bulk modulus (K)

$$K = L - \frac{4}{3}G \quad (5)$$

Young's modulus (Y)

$$Y = (1 + \sigma)2G \quad (6)$$

Fractional bond connectivity (F)

$$F = \frac{4G}{K} \quad (7)$$

Poisson's ratio ( $\sigma$ )

$$\sigma = \frac{(L-2G)}{2(L-G)} \quad (8)$$

Acoustic Impedance (Z)

$$Z = \rho V_1 \quad (9)$$

Microhardness (H)

$$H = \frac{(1-2\sigma)E}{6(1+\sigma)} \quad (10)$$

Debye temperature ( $\theta_D$ )

$$\theta_D = \frac{h}{k_B} \frac{3nN}{4\pi V_m} U_m \quad (11)$$

Where V<sub>m</sub>, k<sub>B</sub>, N, h, U<sub>m</sub>, and n are the molar volume of the sample, Boltzmann's constant, Avogadro number, Planck's constant, mean sound velocity, and many oxygen ions in the sample, respectively.

Mean sound velocity (U<sub>m</sub>)

$$U_m = \left[ \frac{1}{3} \left( \frac{1}{V_1^3} + \frac{2}{V_s^3} \right) \right]^{\frac{1}{3}} \quad (12)$$

Thermal expansion coefficient ( $\alpha_p$ )

$$\alpha_p = 23.2(V_1 - 0.57457) \quad (13)$$

Softening temperature (T<sub>s</sub>)

$$T_s = \left( \frac{M_w}{c_p} \right) V_s^2 \quad (14)$$

Where, M<sub>w</sub> refers molecular weight of the glasses, c is constant equivalent to 1.35 × 10<sup>9</sup> cm<sup>5</sup>·s<sup>-2</sup>·molK<sup>-1</sup>.

### 3. Results and discussion

The experimental values of longitudinal velocity ( $V_L$ ), shear velocity ( $V_S$ ), and density ( $\rho$ ) of the boro-tellurite glass samples for change in  $\text{Eu}_2\text{O}_3$  mol% are tabulated in Table 1. The value of density increased from  $4372 \text{ kg}\cdot\text{m}^{-3}$  to  $4584 \text{ kg}\cdot\text{m}^{-3}$ , while the value of molar volume decreased from  $31.530 \text{ cm}^3$  to  $30.321 \text{ cm}^3$  with a gradual increase of  $\text{Eu}_2\text{O}_3$  concentration in the boro tellurite glasses. The difference in density and molar volume with mol% of europium oxide for the prepared glass system is shown in Figure 2. The density of any glass is the volume of the constituent ions present in the glass network and it is subjected to the number of ions, the nature of ions, and how the ions can move in the structure of the glass. The addition of  $\text{Eu}_2\text{O}_3$  with a higher molecular weight of  $351.926 \text{ g}\cdot\text{mol}^{-1}$  into  $\text{TeO}_2\text{-B}_2\text{O}_3$  having low molecular weight can lead to a rise in the density. Additionally, europium oxide ions reduce the molar volume and result in shrinkage in the glass network, which improves the density. The observed increase in density is endorsed to the rise in the hardness of the glass sample [12,13,33-36]. The linear deviations in density and molar volume of BTE glasses with the rise in the europium oxide content state that the glass network exhibits continuously close-packed.

The longitudinal ultrasonic velocity ( $V_L$ ) and shear ultrasonic velocity ( $V_S$ ) decrease with the increase in the  $\text{Eu}_2\text{O}_3$  concentration as shown in Figure 3. The ultrasonic longitudinal velocity decreases from  $4340 \text{ m}\cdot\text{s}^{-1}$  to  $4015 \text{ m}\cdot\text{s}^{-1}$  whereas ultrasonic shear velocity also decreased from  $2530 \text{ m}\cdot\text{s}^{-1}$  to  $2345 \text{ m}\cdot\text{s}^{-1}$ . This type of decreasing trend in both velocities are might be owing to the flagging in the glass network with an accumulation of  $\text{Eu}_2\text{O}_3$  content into the glass structure and which results in the piercing of O-B-O and Te-O-Te units. Furthermore, splitting of O-B-O and Te-O-Te units reasons the bridging oxygens (BOs) were converted into non-bridging oxygens (NBOs). So there is a reduction in rigidity or weakening of the glass structure [11,14,36].

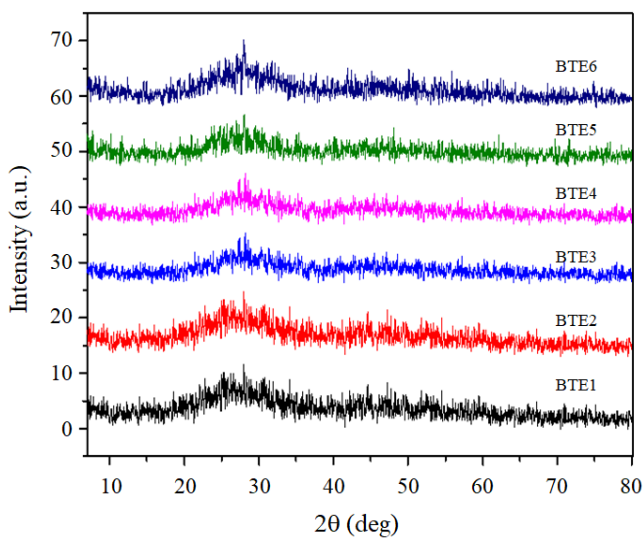


**Figure 1.** Depicts X-ray diffraction spectra of the prepared glass samples. It does not show continuous or discrete sharp peaks but rather a broad halo, revealing the properties of the non-crystalline glass structure.

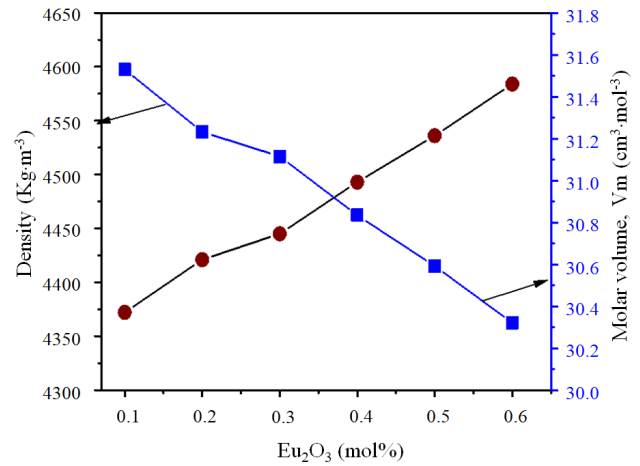


**Figure 2.** Graph of density and molar volume of  $x\text{Eu}_2\text{O}_3\text{-5PbO-25TeO}_2\text{-(70-x)B}_2\text{O}_3$  glasses.

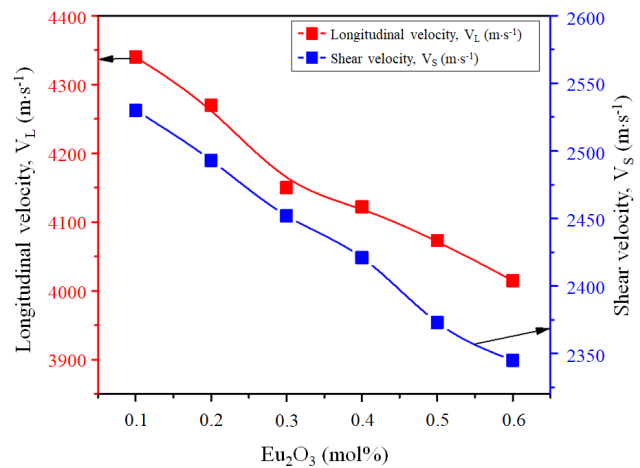


**Figure 3.** Ultrasonic velocity of  $x\text{Eu}_2\text{O}_3\text{-5PbO-25TeO}_2\text{-(70-x)B}_2\text{O}_3$  glasses.

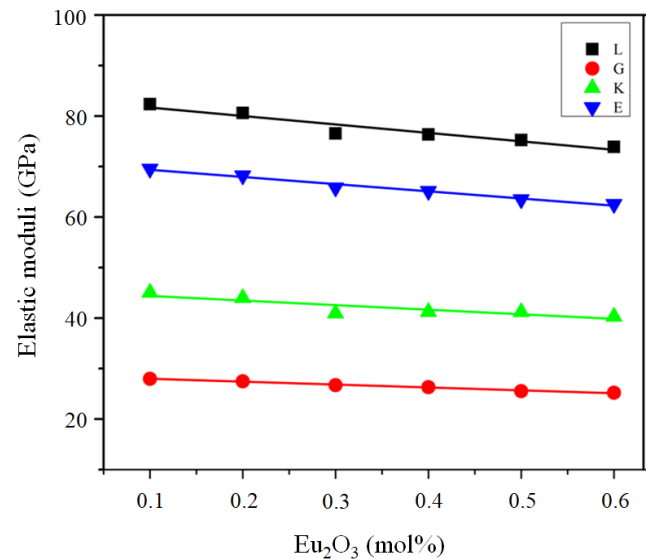


**Figure 4.** Elastic moduli of  $x\text{Eu}_2\text{O}_3\text{-5PbO-25TeO}_2\text{-(70-x)B}_2\text{O}_3$  glasses.

**Table 1.** Values of density ( $\rho$ ), molar volume ( $V_m$ ), ultrasonic velocities ( $V_L$  and  $V_S$ ), and elastic moduli of the specimen.

Specimen ID	Density, $\rho$ ( $\text{kg}\cdot\text{m}^{-3}$ )	Molar volume, $V_m$ ( $\text{cm}^3\cdot\text{mol}^{-1}$ )	Ultrasonic velocity ( $\text{m}\cdot\text{s}^{-1}$ )		Elastic moduli (GPa)			
			Longitudinal, $V_L$	Shear, $V_S$	Longitudinal, L	Shear, G	Bulk, K	Young's, E
BTE1	4372	31.530	4340	2530	82.34	27.98	45.04	69.55
BTE2	4421	31.232	4270	2493	80.61	27.48	43.97	68.22
BTE3	4445	31.115	4150	2452	76.55	26.72	40.92	65.84
BTE4	4493	30.834	4122	2421	76.34	26.33	41.23	65.14
BTE5	4536	30.592	4073	2373	75.25	25.54	41.19	63.50
BTE6	4584	30.321	4015	2345	73.89	25.21	40.29	62.57

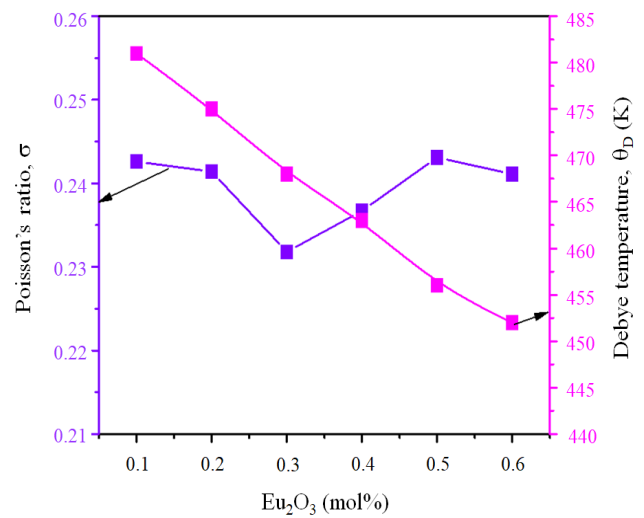
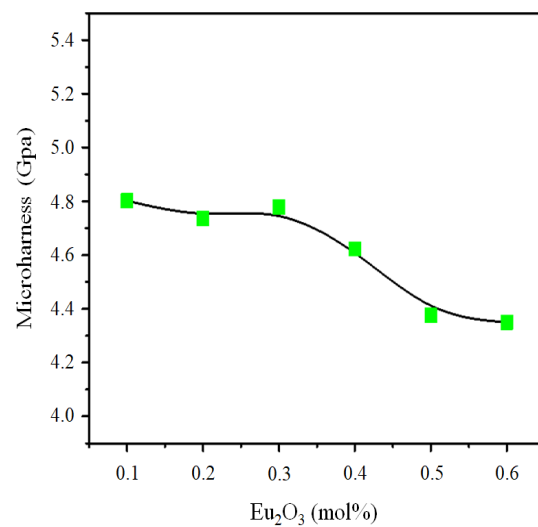
The calculated values of longitudinal modulus (L), shear modulus (G), bulk modulus (K), and Young's modulus (Y) are listed in Table 1. The values show that the elastic moduli reduce with an increase of  $\text{Eu}_2\text{O}_3$  concentration as shown in Figure 4. Longitudinal modulus decreased from 82.34 GPa to 73.89 GPa, shear modulus from 27.98 GPa to 25.21 GPa, bulk modulus from 45.04 GPa to 40.29 GPa, and Young's modulus from 69.55 GPa to 62.57 GPa. The addition of  $\text{Eu}_2\text{O}_3$  concentration produces NBOs, which decrease the rigidity of the BTE glasses, resulting in a decrease of elastic modulus.

As reported in previous work, the Poisson's ratio is influenced by the fluctuations in the cross-link density in the glass structure [4-7]. It is well explained by V Rajendran *et al.* [37] that, Poisson's ratio having values from 0.1 to 0.2 indicates the high cross-link density whereas Poisson's ratio values ranging from 0.3 to 0.5 exhibit low cross-link density. But the Poisson's ratio values of BTE glasses come in the range of 0.2318 to 0.2426 (Figure 5) showing the presence of low cross-link densities. The measured fractional bond connectivity values vary from 2.486 to 2.612 as shown in Figure 7 and these values also support [37] the presence of low cross-link density in BTE glasses. This low cross-link density could be owing to significant structural changes originated by the insertion of  $\text{Eu}_2\text{O}_3$  content into the borotellurite glass network [36].

In addition, as stated by Srivastava and Srinivasan *et al.*, [38], the important parameter, microhardness (H), describes the stress required to remove the free volume inside the glasses, and the other parameter, the thermal expansion coefficient of materials depends on the strength of bonds. The free volume in the glasses gives a fact of openness in the glasses which is the characteristic nature of glasses having consistent structure. Figure 6, shows the reduction in microhardness and which reveals the presence of non-bridging oxygen ion (NBO) and this causes the formation of a soft glassy network [39-42]. For solid materials, Debye temperature ( $\theta_D$ ) is another vital parameter, which relates the atomic vibrations. Also, it characterizes the temperature at which all types of vibrations are excited [18-20, 43-46]. Figure 7 shows the reducing behavior of the Debye temperature indicating the weakening of the structure and the reduction of the rigidity of the glass systems. The reduction in Debye temperature in BTE glasses is mostly attributed to the alteration in the number of atoms per unit volume and the presence of NBOs. [22-25, 43-46].

The values of thermal expansion coefficient ( $\alpha_p$ ), acoustic impedance (Z), and softening temperature ( $T_s$ ) are listed in Table 2. These values reduce with the mole% of the doped  $\text{Eu}_2\text{O}_3$  content in a  $\text{TeO}_2\text{-B}_2\text{O}_3$  glass sample. The acoustic impedance values decrease from  $1.8974 \text{ kg}\cdot\text{m}^{-2}\text{s}^{-1}$  to  $1.8404 \text{ kg}\cdot\text{m}^{-2}\text{s}^{-1}$ , thermal expansion coefficient

( $\alpha_p$ ) values decrease from  $100674.7 \alpha_p\cdot(\text{K}^{-1})$  to  $93134.67 \alpha_p\cdot(\text{K}^{-1})$  as shown in Figure 8, and softening temperature ( $T_s$ ) values decrease from 2875.52 K to 2595.28 K. This has led to a decrease in the rigidity and compactness of the glass structure [4,47]. This decreasing trend confirms the rigidity of the glass structure and the weakening of the glass network in the system.

**Figure 5.** A graph of Poisson's ratio and Debye temperature of  $x\text{Eu}_2\text{O}_3\text{-5PbO-25TeO}_2\text{-(70-x) B}_2\text{O}_3$  Glasses.**Figure 6.** Microhardness of  $x\text{Eu}_2\text{O}_3\text{-5PbO-25TeO}_2\text{-(70-x) B}_2\text{O}_3$  Glasses.

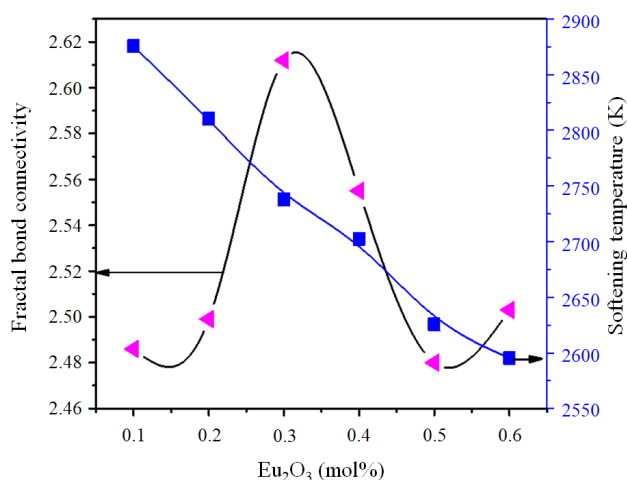


**Figure 7.** Fractional bond connectivity and Softening temperature of  $x\text{Eu}_2\text{O}_3$ - $5\text{PbO}$ - $25\text{TeO}_2$ - $(70-x)\text{B}_2\text{O}_3$  Glasses.

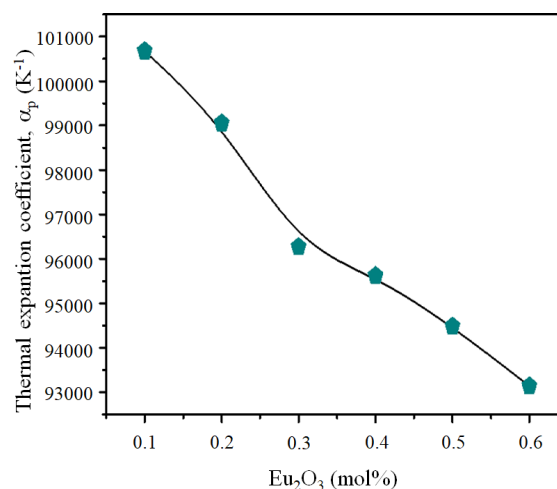


**Figure 8.** Thermal expansion coefficient of  $x\text{Eu}_2\text{O}_3$ - $5\text{PbO}$ - $25\text{TeO}_2$ - $(70-x)\text{B}_2\text{O}_3$  Glasses.

**Table 2.** Values of fractional bond connectivity (F), Acoustic Impedance (Z), Poisson's ratio( $\sigma$ ), Microhardness (H), Thermal expansion coefficient ( $\alpha_p$ ), Debye temperature ( $\theta_D$ ), and Softening temperature ( $T_s$ ) of glass systems.

Specimen ID	Fractional bond connectivity (F)	Poisson's ratio, $\sigma$	Acoustic Impedance, Z ( $\times 10^7 \text{ kg}\cdot\text{m}^{-2}\cdot\text{s}^{-1}$ )	Micro hardness, H ( $\times 10^9 \text{ N}\cdot\text{m}^{-2}$ )	Debye temperature, $\theta_D$ (K)	Thermal expansion coefficient, $\alpha_p$ ( $\text{K}^{-1}$ )	Softening temperature, $T_s$ (K)
BTE1	2.486	0.2426	1.8974	4.802	481	100674.7	2875.52
BTE2	2.499	0.2414	1.8877	4.737	475	99050.67	2810.33
BTE3	2.612	0.2318	1.8447	4.778	468	96266.67	2737.93
BTE4	2.555	0.2367	1.8520	4.623	463	95617.07	2702.41
BTE5	2.480	0.2431	1.8475	4.375	456	94480.27	2625.48
BTE6	2.503	0.2411	1.8404	4.350	452	93134.67	2595.28

#### 4. Conclusions

The  $x\text{Eu}_2\text{O}_3$ - $5\text{PbO}$ - $25\text{TeO}_2$ - $(70-x)\text{B}_2\text{O}_3$  glasses were ready by the melt quenching method. The amorphous behavior of glass was found by using X-ray diffraction. The density of glasses at room temperature was increased almost linearly from  $4372 \text{ kg}\cdot\text{m}^{-3}$  to  $4584 \text{ kg}\cdot\text{m}^{-3}$  and the molar volume of the glasses decreased linearly from  $31.530 \text{ cm}^3$  to  $30.321 \text{ cm}^3$  as function of  $\text{Eu}_2\text{O}_3$  concentration due to the addition of  $\text{Eu}_2\text{O}_3$  with a higher molecular weight of  $351.926 \text{ g}\cdot\text{mol}^{-1}$  into  $\text{TeO}_2$ - $\text{B}_2\text{O}_3$  having low molecular weight. The decrease of elastic moduli indicates the loose packing structure in the glass network therefore the rigidity and velocities are reduced. The Debye temperature, softening temperature, microhardness, and thermal expansion coefficient decreases as  $\text{Eu}_2\text{O}_3$  content increases is attributed to considerable weakening in the glass structure due to non-bridging oxygen bonds, hence rigidity of the glass structure decreases. The variation in Poisson's ratio and fractional bond connectivity reveals the existing glasses contain a low cross-link density.

#### Acknowledgments

The authors thank the Department of Physics, Bangalore University, Bengaluru for providing the necessary experimental setup for the ultrasonic measurements of glass samples.

#### References

- [1] B. Eraiah, and R. V. Anavekar, "Elastic properties of silver-phospho-vanadate glasses," *Journal of Alloys and Compounds*, vol. 489, pp. 325-327, 2010.
- [2] T. Rouxel, "Elastic properties and short-to medium-range order in glasses," *Journal of American Ceramic Society*, vol. 90, pp. 3019-3039, 2007.
- [3] M. K. Halimah, W. M. Daud, and H. A. A. Sidek, "Effect of AgI addition on elastic properties of quaternary tellurite glass systems," *Chalcogenide Letters*, vol. 7, pp. 613-620, 2010.
- [4] S. Thirumaran, and R. Palani, "Elastic and mechanical properties of glass specimen by ultrasonic method," *ARPJ Journal of Engineering and Applied Sciences*, vol. 4, pp. 27-31, 2009.
- [5] J. S. Lee, H. S. Oh, W. Kim, C. W. Ryu, J. Y. Kim, H. J. Chang, J. L. Gu, K. F. Yao, B. S. Murty, and E. S. Park, "Anomalous behavior of glass-forming ability and mechanical response in a series of equiatomic binary to denary metallic glasses," *Materialia*, vol. 9, p.100505, 2020.
- [6] M. Deraud, and J. Y. Prieur, "Ultrasonic Study of Lithium Borate Glasses," *Journal de Physique Colloques*, vol. 43, pp. 497-500, 1982.
- [7] T. Sumathi, and A. N. Kannappan, "Ultrasonic Investigation on Sodium and Calcium Tungsten Phosphate Glass System," *Research Journal of Chemical Sciences*, vol. 2, pp.14-17, 2012.

- [8] N. S. A. El-aal, "Elastic Properties of  $\gamma$ -radiated Borate Glasses Using Pulse-Echo Technique," *Egypt Journal of Solids*, vol. 24, pp. 181-192, 2001.
- [9] C. N. Reddy, and R. V. Anavekar, "Elastic properties and spectroscopic studies of  $\text{Li}_2\text{O}-\text{B}_2\text{O}_3-\text{V}_2\text{O}_5$  glasses," *Material Chemistry and Physics*, vol. 112, pp. 359-365, 2008.
- [10] G. El-Damrawi, A. M. Abdelghany, M. I. Abdelghany, and M. A. Marshal, "Structural role of chromium sulfate in modified borate glasses and glass ceramics," *Materialia*, vol. 16, p. 101095, 2021.
- [11] P. Naresh, A. Padmaja, and K. Siva Kumar, "Influence of Zinc oxide addition on the biological activity and electrical transport properties of  $\text{TeO}_2-\text{Li}_2\text{O}-\text{B}_2\text{O}_3$  glasses," *Materialia*, vol. 9, p. 100575, 2020.
- [12] Y. Yamsuk, P. Yasaka, J. Kaewkhao, and N Sangwanateee, " $\text{Sm}^{3+}$  ions doped zinc barium tellurite oxyfluoride glasses for laser materials," *Journal of Metals, Materials and Minerals*, vol. 30, pp. 86-93, 2020.
- [13] C. Devaraja, G. V. Jagadeesha Gowda, B. Eraiah, G. Devarajulu, and G. Jagannath, "Physical, structural and photoluminescence properties of lead boro-tellurite glasses doped with  $\text{Eu}^{3+}$  ions," *Vacuum*, vol. 177, p. 109426, 2020.
- [14] C. Devaraja, G. V. Jagadeesha Gowda, and B. Eraiah, "FTIR and Raman studies of  $\text{Eu}^{3+}$  ions doped alkali boro tellurite glasses," *AIP Conference Proceedings*, vol. 2115, pp. 1-5, 2019.
- [15] R. Rajaramakrishna, C. Wongdeeying, P. Yasaka, P. Limkitjaroenpom, N. Sangwanateee, and J. Kaewkhao, " $\text{Pr}^{3+}$  doped  $\text{BaO}:\text{ZnO}:\text{B}_2\text{O}_3:\text{TeO}_2$  glasses for laser host matrix," *Journal of Metals, Materials and Minerals*, vol. 28, no. 2, pp. 47-54, 2019.
- [16] S. Kaur, N. Deopa, A. Prasad, R. Bajaj, and A.S. Rao, "Intense green emission from  $\text{Tb}^{3+}$  ions doped zinc-lead alumino borate glasses for laser and w-LEDs applications," *Optical Materials*, vol. 84, pp. 318-323, 2018.
- [17] E. S. Yousef, M. M. Elokr, and Y. M. Aboudeif, "Optical, elastic properties and DTA of TNZP host tellurite glasses doped with  $\text{Er}^{3+}$  ions," *Journal of Molecular Structure*, vol. 1108, pp. 257-262, 2016.
- [18] S. A. Saleem, B. C. Jamalaiah, A. M. Babu, K. Pavani, and L. R. Moorthy, "A study on fluorescence properties of  $\text{Eu}^{3+}$  ions in alkali lead tellurofluoroborate glasses," *Journal of Rare Earths*, vol. 28, pp. 189-193, 2010.
- [19] P. S. Wong, M. H. Wan, R. Hussin, H. O. Lintang, and S. Endud, "Structural and luminescence studies of europium ions in lithium aluminium borophosphate glasses," *Journal of Rare Earths*, vol. 32, pp. 585-592, 2014.
- [20] A. Madhu, B. Eraiah, P. Manasa, and N. Srinatha, " $\text{Nd}^{3+}$ -doped lanthanum lead boro-tellurite glass for lasing and amplification applications," *Optical Materials*, vol. 75, pp. 357-366, 2018.
- [21] T. Hasegawa, "Optical properties of  $\text{Bi}_2\text{O}_3-\text{TeO}_2-\text{B}_2\text{O}_3$  glasses," *Journal of Non-Crystalline Solids*, vol. 357, pp. 2857-2862, 2011.
- [22] R. Rajaramakrishna, R. Lakshmi kantha, and R. V. Anavekar, "Elastic properties of  $\text{Li}^+$  doped lead zinc borate glasses," *AIP Conference Proceedings*, vol. 1591, pp. 736-738, 2014.
- [23] G. V. Jagadeesha Gowda, and B. Eraiah, "Elastic properties of silver borate glasses doped with praseodymium oxide," *AIP Conference Proceedings*, vol. 724, pp. 722-724, 2014.
- [24] K. Maheshvaran, and K. Marimuthu, "Concentration-dependent  $\text{Eu}^{3+}$  doped boro-tellurite glasses structural and optical investigations," *Journal of Luminescence*, vol. 132, p. 2259, 2012.
- [25] M. Kumar, T. K. Seshagiri, and S. V. Godbole, "Fluorescence lifetime and Judd-Ofelt parameters of  $\text{Eu}^{3+}$  doped  $\text{SrBPO}_5$ ," *Physica B: Condensed Matter*, vol. 410, p. 141, 2013.
- [26] P. A. Azeem, M. Kalidasan, and K. Rama Gopal, and R. R. Reddy, "Spectral analysis of  $\text{Eu}^{3+}:\text{B}_2\text{O}_3-\text{Al}_2\text{O}_3-\text{mF}_2$  ( $\text{m}=\text{Zn}$ ,  $\text{Ca}$ ,  $\text{Pb}$ ) glasses," *Journal of Alloys and Compounds*, vol. 474, p. 536, 2009.
- [27] K. Marimuthu, R. T. Karunakaran, S. Surendra Babu, G. Muralidharan, S. Arumugam, and C. K. Jayasankar, "Structural and spectroscopic investigations on  $\text{Eu}^{3+}$  doped alkali fluoroborate glasses," *Solid State Science*, vol. 11, p. 1297, 2009.
- [28] W. Stambouli, H. Elhouichet, B. Gelloz, and M. Ferid, "Optical and spectroscopic properties of Eu-doped tellurite glasses and glass ceramics," *Journal of luminescence*, vol. 138, pp. 201-208, 2013.
- [29] V. Dimitrov, and T. Komatsu "An interpretation of optical properties of oxides and oxide glasses in terms of the electronic polarizability and average single bond strength," *Journal of the University of Chemical Technology and Metallurgy*, vol. 45, pp. 219-250, 2010.
- [30] Y. S. Rammah, I. O. Olarinoye, F. I. El-Agawany, A. El-Adawy, A. Gamal, and E. S. Yousef, "Elastic moduli, photon, neutron, and proton shielding parameters of tellurite bismo-vanadate ( $\text{TeO}_2-\text{V}_2\text{O}_5-\text{Bi}_2\text{O}_3$ ) semiconductor glasses," *Ceramic International*, vol. 46, pp. 25440-25452, 2020.
- [31] B. Eraiah, M. G. Smitha, and R. V. Anavekar, "Elastic properties of lead-phosphate glasses doped with samarium trioxide," *Journal of Physics and Chemistry of Solids*, vol. 71, pp. 153-155, 2010.
- [32] D. Souri, "Ultrasonic velocities, elastic modulus and hardness of ternary  $\text{Sb}-\text{V}_2\text{O}_5-\text{TeO}_2$  glasses," *Journal of Non-Crystalline Solids*, vol. 470, pp. 112-121, 2017.
- [33] S. Kaur, O. P. Pandey, C. K. Jayasankar, and N. Chopra, "Influence of heat treatment on spectroscopic and structural properties of vitreous  $\text{Er}^{3+}$ -doped zinc boro-tellurite," *Journal of Non-Crystalline Solids*, vol. 530, p. 119842, 2020.
- [34] K. S. Shaaban, A. M. Ali, Y. B. Saddeek, K. A. Aly, A. Dahshan, and S. A. Amin, "Synthesis, Mechanical and Optical Features of  $\text{Dy}_2\text{O}_3$  Doped Lead Alkali Borosilicate Glasses," *Silicon*, vol. 11, pp. 1853-1861, 2019.
- [35] M. R. Dousti, "Enhanced luminescence properties of  $\text{Nd}^{3+}$  doped boro-tellurite glasses via silver additive," *Optik*, vol. 136, pp. 553-557, 2017.
- [36] G. V. J. Gowda, C. Devaraja, B. Eraiah, A. Dahshan, and S. N. Nazrin, Structural, thermal and spectroscopic studies of Europium trioxide doped lead boro-tellurite glasses, *Journal of Alloys and Compounds*, vol. 871, p. 159585, 2021.

- [37] V. Rajendran, N. Palanivelu, B. K. Chaudhuri, and K. Goswami, "Characterisation of semiconducting  $V_2O_5$ - $Bi_2O_3$ - $TeO_2$  glasses through ultrasonic measurements," *Journal of Non-Crystalline Solids*, vol. 320, pp. 195-209, 2003.
- [38] S. C. Srivastava C M, "Science of Engineering Materials," 2<sup>nd</sup> edition, *New Age International (p) Limited*, New Delhi, 1997.
- [39] R. El-Mallawany, A. El Adawy, A. Gamal, and Y. S. Rammah, "Experimental and theoretical elastic moduli of sodium–zinc–tellurite glasses," *Optik*, vol. 243, p.167330, 2021.
- [40] R. El-Mallawany, M. D. Abdalla, and I. A. Ahmed, New tellurite glass: Optical properties, *Material Chemistry and Physics*, vol. 109, pp. 291-296, 2008.
- [41] S. N. Nazrin, M. K. Halimah, A. A. A. Awshah, S. P. Yee, L. Hasnimulyati, I. Boukhris, G. V. Jagadeesha Gowda, M. N. Azlan, J. L. Clabel H, and S. N. Nadzim, "Experimental and theoretical elastic studies on neodymium-doped zinc tellurite glasses," *Journal of Non-Crystalline Solids*, vol. 575, p. 121208, 2022.
- [42] R. El-Mallawany, and I. A. Ahmed, "Thermal properties of multicomponent tellurite glass," *Journal of Material Science*, vol. 43, pp. 5131-5138, 2008.
- [43] M. K. Halimah, S. A. Umar, K. T. Chan, A. A. Latif, M. N. Azlan, A. I. Abubakar, and A. M. Hamza, "Study of rice husk silicate effects on the elastic, physical and structural properties of borotellurite glasses," *Material Chemistry and Physics*, vol. 238, p. 121891, 2019.
- [44] R. A. Tafida, M. K. Halimah, F. D. Muhammad, K. T. Chan, M. Y. Onimisi, A. Usman, A. M. Hamza, and S. A. Umar, "Structural, optical and elastic properties of silver oxide incorporated zinc tellurite glass system doped with  $Sm^{3+}$  ions," *Material Chemistry and Physics*, vol. 246, p. 122801, 2020.
- [45] V. C. Veeranna Gowda, C. Narayana Reddy, K. C. Radha, R. V. Anavekar, J. Etourneau, and K. J. Rao, "Structural investigations of sodium diborate glasses containing  $PbO$ ,  $Bi_2O_3$  and  $TeO_2$ : Elastic property measurements and spectroscopic studies," *Journal of Non-Crystalline Solids*, vol. 353, pp. 1150-1163, 2007.
- [46] B. Bridge, N. D. Patel, and D. N. Waters, "On the elastic constants and structure of the pure inorganic oxide glasses," *Physica Status Solidi (a)*, vol. 77, pp. 655-668, 1983.
- [47] R. Palani, and J. Selvarasi, "Elastic and structural properties of potassium and calcium-doped borate lithium glasses," *International Journals of Current Research Reviews*, vol. 9, pp.71-79, 2017.